

## The Atomic and Electronic Structure Changes Upon Delithiation of LiCoO<sub>2</sub>: From First Principles Calculations

F. Xiong<sup>1</sup>, H. J. Yan<sup>1</sup>, Y. Chen<sup>1</sup>, B. Xu<sup>1,2</sup>, J. X. Le<sup>1</sup>, C. Y. Ouyang<sup>1,2\*</sup>

<sup>1</sup> Department of Physics, Jiangxi Normal University, Nanchang 330022, China

<sup>2</sup> Key Laboratory for Advanced Functional materials of Jiangxi Province, Nanchang, 330022, China

\*E-mail: [cyouyang@jxnu.edu.cn](mailto:cyouyang@jxnu.edu.cn)

Received: 2 August 2012 / Accepted: 2 September 2012 / Published: 1 October 2012

The physical origin of the degradation on the cycling performance of LiCoO<sub>2</sub> upon deep lithium extraction is studied from first principles calculations. Results show that the structural stability is strongly associated with the electronic structures of Co-3d, which is very flexible and can be exhibited as different electronic configurations. In LiCoO<sub>2</sub>, Co<sup>3+</sup> is non-magnetic and holds the (t<sub>2g</sub>↑)<sup>3</sup>(t<sub>2g</sub>↓)<sup>3</sup> electronic configuration. Upon lithium deintercalation, some Co<sup>3+</sup> ions loss one electron and become Co<sup>4+</sup> with (t<sub>2g</sub>↑)<sup>3</sup>(t<sub>2g</sub>↓)<sup>2</sup> configuration. Both structures are stable since the distortion of the CoO<sub>6</sub> octahedral is small, and thus these structures do not contribute much to the instability. On the other hand, oxygen vacancy is one important reason to the structural instability. We found that spin flip occurs to the electronic structure of Co-3d close to oxygen vacancies. Co<sup>3+</sup> holds the (↑)<sup>4</sup>(↓)<sup>2</sup> electronic configuration and magnetized with 2 μ<sub>B</sub> magnetic moment. Furthermore, some Co<sup>3+</sup> obtains one electron and becomes Co<sup>2+</sup> near the oxygen vacancy. In these cases, the charge distribution around the Co atom is not symmetric and the local structure is distorted obviously, which can further accelerate the process of the structural degradation.

**Keywords:** Lithium ion batteries; High voltage charging; Structural stability; Li<sub>x</sub>CoO<sub>2</sub>; Electronic structure

### 1. INTRODUCTION

Materials for cathodes in lithium rechargeable batteries have been widely studied in the last three decades. The energy density is still a big problem for wide application of lithium ion batteries in the electrical vehicle. Among various cathodes materials studied, LiCoO<sub>2</sub> is the most widely used in the lithium ion battery industry [1, 2]. LiCoO<sub>2</sub> has a theoretical capacity of about 270 mAhg<sup>-1</sup> when all Li atoms are extracted from the material, while the practical capacity achieves only 130–150 mAhg<sup>-1</sup> [3], indicating that only half of the Li atoms can be used during the charge/discharge process.

In order to improve the energy density of lithium ion batteries, we can improve either the capacity or the intercalation potential of the cathode material. Both of them can be achieved simply by extracting more Li from the  $\text{LiCoO}_2$  lattice. However, the structural stability of the  $\text{LiCoO}_2$  material is very bad during the charge/discharge cycling when more than half of the Li atoms are extracted, which leads to poor cycling performance of the battery. Furthermore, high voltage charging of the material is also harmful to the safety of the battery, because  $\text{O}_2$  gas will be released from the lattice accompanied by structural transition upon high voltage charging, and then reacts with the electrolyte. Experiments have shown that oxide coating layers like  $\text{Al}_2\text{O}_3$ ,  $\text{ZrO}_2$ ,  $\text{MgO}$ , et al, can improve the structural stability and thus the cycling performance [4-7]. However, the physical mechanism behind this improved performance is still not clear to the literature. Oxides coating affects only the surface properties of the material, it is hard to understand how the surface effect induced the bulk structural stability.

In order to understand the mechanism of the oxygen release problem in  $\text{LiCoO}_2$  during the charge/discharge process, it is important to understand the basic physical and chemical changes of the materials upon lithium deintercalation. Experimentally, *in situ* synchrotron X-ray diffraction is applied to observe the structural change of the material during cycling [8]. It is found that the phase transition upon high voltage charging of  $\text{Al}_2\text{O}_3$  coated  $\text{LiCoO}_2$  is reversible. Unfortunately, it is not easy to observe the microscopic structure change and local electronic structure change from those *in situ* experiments. Therefore, theoretical studies are important to reveal the physical mechanism of the coating improved cycling performance.

The physical and chemical properties like electronic structures [9-10], lithium ion diffusion [11], lithium ion ordering and phase stability, voltage-temperature phase diagram et al. [12] of the partly delithiated  $\text{Li}_x\text{CoO}_2$  is studied with first principles calculations in the past. However, those studies did not give reasonable predictions to the electronic and magnetic ground states of this material. Co is nonmagnetic in stoichiometrical  $\text{LiCoO}_2$ , as the average oxidation state of the cobalt is  $\text{Co}^{3+}$  with 6 electrons taking the 3d-orbital. In an octahedral crystal field, 3d-orbital split into  $t_{2g}$  triplet and  $e_g$  doublet. Therefore, both spin up and spin down of the  $t_{2g}$  triplet is fully filled by the 6 electrons in  $\text{LiCoO}_2$ , which gives rise to a symmetric distribution of the charge around the  $\text{CoO}_6$  octahedral. However, upon delithiation of the  $\text{LiCoO}_2$ , the average oxidation state of Co is higher than +3. Therefore, some Co atoms become  $\text{Co}^{4+}$  and the others remain  $\text{Co}^{3+}$ . Experimentally, it is shown that delithiated  $\text{Li}_x\text{CoO}_2$  ( $x < 1$ ) exhibits magnetic ground state, indicating that the charge distribution in the spin up and spin down channels are no longer symmetric. However, conventional local density approximation (LDA) or general gradient approximation (GGA) level of the calculation results in non-magnetic solution of the ground state [9-12] and thus a metallic electronic structure, which is not consistent with the experimental observations.

More recently, within the density functional theory (DFT) scheme, GGA+U (or LDA+U) method, in which a Hubbard U term is added to describe the orbital dependence of the Coulomb and exchange interaction[13, 14], is shown to give much better description of the electronic structure in oxide cathode materials for lithium ion batteries [15-18]. In the present work, we show that GGA+U also gives good description of the electronic ground state of  $\text{Li}_x\text{CoO}_2$  ( $x < 1$ ). Then, we focus on the electronic and magnetic state changes upon lithium deintercalation process and oxygen release in

$\text{Li}_x\text{CoO}_2$ , and we demonstrate that the Co spin state change in  $\text{Li}_x\text{CoO}_2$  ( $x=1, 0.75, 0.5$  and  $0.25$ ) is associated with the local structural distortion and thus the structural stability.

## 2. COMPUTATIONAL DETAILS

All calculations in the present study are performed at GGA+U level, with the projector augmented wave (PAW) method [19] as implemented in the Vienna *ab initio* simulation package (VASP) [20]. The U (the on-site coulomb term) value for the Co-3d state is selected to be 4.91 eV according to other reports [17, 21], and our tested results show that this value is suitable for the  $\text{Li}_x\text{CoO}_2$  system.

All calculations are performed with a  $2 \times 2 \times 1$  super cell containing 12 formula units (12Li, 12Co and 24O). The convergence tests of the total energy with respect to the k-points sampling and cut-off energy have been carefully examined, which ensure that the total energy is converged to within  $10^{-5}$  eV per formula unit. The Monkhorst-Pack [22] scheme  $3 \times 3 \times 1$   $k$ -points mesh is used for the integration in the irreducible Brillouin zone. Energy cut-off for the plane waves is chosen to be 520 eV. Before the calculation of the electronic structure, both the lattice parameters and the ionic position are fully relaxed, and the final forces on all relaxed atoms are less than  $0.005 \text{ eV}\text{\AA}^{-1}$ . In all the calculations, spin polarization is included because the magnetic atoms play important roles in the electronic structure. The calculation of the density of states (DOS) is smeared by the Gaussian smearing method with a smearing width of 0.05 eV.

## 3. RESULTS AND DISCUSSION

### 3.1 The structure changes upon delithiation

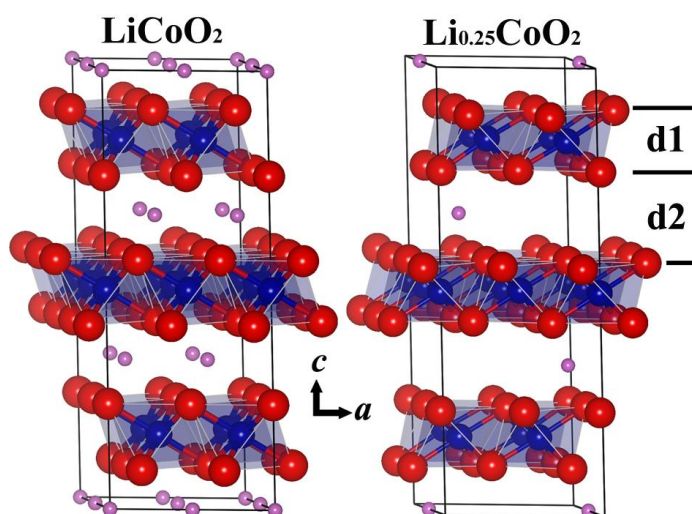


**Figure 1.** Schematic views of the atomic structures of  $\text{LiCoO}_2$  and  $\text{Li}_{0.25}\text{CoO}_2$  in the ball and stick mode. The large (red), middle-sized (blue), and small (purple) spheres are O, Co and Li atoms, respectively. The transparent polyhedral are  $\text{CoO}_6$  octahedral. Symbols “d1” and “d2” are the O-O interlayer distance, “a” and “c” refer to the orientation of the lattice vectors.

LiCoO<sub>2</sub> is isostructural with  $\alpha$ -NaFeO<sub>2</sub>, whose space group is  $R\bar{3}m$ . Within this space group, Li occupies the 3a, Co the 3b, and O the 6c sites. It has an ordered rock salt structure in which alternate layers of Li and Co atoms occupy octahedral sites within the face centered cubic oxide array [23-24]. Figure 1 gives the relaxed structures of LiCoO<sub>2</sub> and Li<sub>0.25</sub>CoO<sub>2</sub>. In general, we found that the CoO<sub>6</sub> octahedral is kept unchanged upon delithiation, even when three fourth of Li atoms are removed from the lattice, except for certain small distortion.

**Table 1.** The relaxed structural parameters of Li<sub>x</sub>CoO<sub>2</sub>. The “d1” and “d2” correspond to the average O-O interlayer distance shown in Fig. 1

System	Lattice parameters (Å)		Volume (Å <sup>3</sup> )	Oxygen interlayer distance (Å)	
				d1	d2
LiCoO <sub>2</sub>	$a=b=5.6738$ $c=14.1670$	$\alpha=\beta=90.00^\circ$ $\gamma=120.00^\circ$	395.11	2.0657	2.6566
Li <sub>0.75</sub> CoO <sub>2</sub>	$a=5.6975$ $b=5.6926$ $c=14.3781$	$\alpha=89.78^\circ$ $\beta=89.99^\circ$ $\gamma=119.98^\circ$	403.95	2.0277	2.7564
Li <sub>0.5</sub> CoO <sub>2</sub>	$a=5.6775$ $b=5.6839$ $c=14.6222$	$\alpha=89.42^\circ$ $\beta=89.98^\circ$ $\gamma=120.11^\circ$	408.15	1.9355	2.9049
Li <sub>0.25</sub> CoO <sub>2</sub>	$a=5.6735$ $b=5.6723$ $c=15.0530$	$\alpha=89.53^\circ$ $\beta=90.46^\circ$ $\gamma=120.03^\circ$	419.40	1.9079	3.1186
<sup>a)</sup> LiCoO <sub>2</sub>	$a=b=2.8156$ $c=14.0542$	$\alpha=\beta=90^\circ$ $\gamma=120^\circ$	96.49	2.8156	3.0940
<sup>a)</sup> Li <sub>0.68</sub> CoO <sub>2</sub>	$a=b=2.8107$ $c=14.2235$	$\alpha=\beta=90^\circ$ $\gamma=120^\circ$	97.31	2.8107	3.1782
<sup>a)</sup> Li <sub>0.48</sub> CoO <sub>2</sub>	$a=b=2.8090$ $c=14.3890$	$\alpha=\beta=90^\circ$ $\gamma=120^\circ$	98.33	2.8090	3.2553
<sup>a)</sup> Li <sub>0.35</sub> CoO <sub>2</sub>	$a=b=2.8070$ $c=14.3890$	$\alpha=\beta=90^\circ$ $\gamma=120^\circ$	98.51	2.8070	3.2856

a). Experimental results from reference [25].

Detailed structural information is listed in Table 1, together with the experimental values [25]. These calculated lattice constants are basically in agreement with experimental values, although over estimated to some extent. The lattice parameters  $a$  and  $b$  do not change significantly while  $c$  increases when the lithium ions are extracted from the electrode. In the stoichiometric LiCoO<sub>2</sub>, the lattice parameters  $a$  and  $b$  are the same. However, small difference between  $a$  and  $b$  is obtained from the calculation when part of Li atoms are removed from the lattice. This is simply due to the distribution of the remaining Li atoms in the lattice is not symmetric with our small unit cell. In a macroscopic case, when Li atoms are distributed evenly in the lattice, this lattice parameter difference between  $a$  and  $b$  will be disappeared. The reason for the difference in  $\alpha$  and  $\beta$  for the delithiated cases is the same. For the expanded lattice along the  $c$ -vector direction when lithium is partly removed, we believe it is due to

the weakened coulomb interaction between positively charged Li layers and negatively charged  $\text{CoO}_6$  layers. In fact, the binding forces in the layered  $\text{LiCoO}_2$  material include the coulomb interactions between Li layers and  $\text{CoO}_6$  layers and Van der Waals interaction between  $\text{CoO}_6$  layers. When there are more Li ions in the lattice, the binding forces are dominated by the coulomb interaction. Therefore, when Li content is lowered during delithiation, the interaction strength is lowered and the lattice is expanded along the  $c$ -axis direction. When the lithium content is very low (or completely removed), the binding forces are dominated by the Van der Waals interaction. In this case, the system comes to a new and shortened equilibrium layer to layer distance. At the same time, the O-O interlayer distances also change substantially upon lithium extraction. The “d1”, which is 2.066 Å in  $\text{LiCoO}_2$ , is shortened by near 0.16 Å, to the value of 1.908 Å in  $\text{Li}_{0.25}\text{CoO}_2$ . The thickness of Co-O layer becomes thinner indicates that the Co-O bonds becomes stronger. On the other hand, the “d2” is elongated substantially from 2.657 Å in  $\text{LiCoO}_2$  to 3.119 Å in  $\text{Li}_{0.25}\text{CoO}_2$ , indicating that the layer to layer interaction becomes weaker. These results are in good agreement with experimental findings [25].

### 3.2. Average delithiation potential

To enhance the energy density of the  $\text{LiCoO}_2$  material, it is suggested to charge the battery to a higher voltage and extract more Li from the cathode. Here we calculated the average intercalation potential of the  $\text{Li}_x\text{CoO}_2$  material at different stage. The average lithium extraction potential is calculated by: [12, 26]:

$$V_{\text{ave}} = -\Delta G/nF$$

Where  $\Delta G$  is the Gibbs free energy changes for the removal reaction,  $F$  is the Faraday constant, and  $n$  is the Mole number of lithium ions removed. Generally, it is assumed that the changes in volume and entropy are small during the reaction. Therefore, the average removal potential can be approximately obtained from the internal energy given by:

$$V_{\text{ave}} = -\Delta E/nF$$

where  $\Delta E$  is the calculated difference of the total energy. Here, the potential is examined by the composition ranges. As for the energy changes of removal between  $\text{LiCoO}_2$  and  $\text{Li}_x\text{CoO}_2$ ,  $\Delta E$  is given by:

$$\Delta E = E[\text{LiCoO}_2] - E[\text{Li}_x\text{CoO}_2] - (1-x) E_{\text{bcc}}[\text{Li}]$$

Where  $E_{\text{tot}}[\text{LiCoO}_2]$  and  $E_{\text{tot}}[\text{Li}_x\text{CoO}_2]$  are the total energy of  $\text{LiCoO}_2$  and  $\text{Li}_x\text{CoO}_2$ , and  $E_{\text{bcc}}[\text{Li}]$  is the total energy of metallic lithium in a body-centered-cubic (bcc) phase.

The predicted average intercalation potential is ~3.78 V when half number of the Li is removed from the material. This is a little bit lower than the experimental charge/discharge potential plateau of

~4.0 V [5, 8]. This underestimated potential is also reported in other materials, which is attributed to the underestimation of the cohesive energy of metallic lithium as reference electrode [26-27]. Upon further removal of lithium ions from the  $\text{Li}_{0.5}\text{CoO}_2$  state to the  $\text{Li}_{0.25}\text{CoO}_2$  state, the average intercalation potential is increased to 3.95 V. Although this value is also lower than the experimental value of ~4.2 V, the amount of the increased potential value is similar for the theoretical and experimental values.

### 3.3 Electronic structure

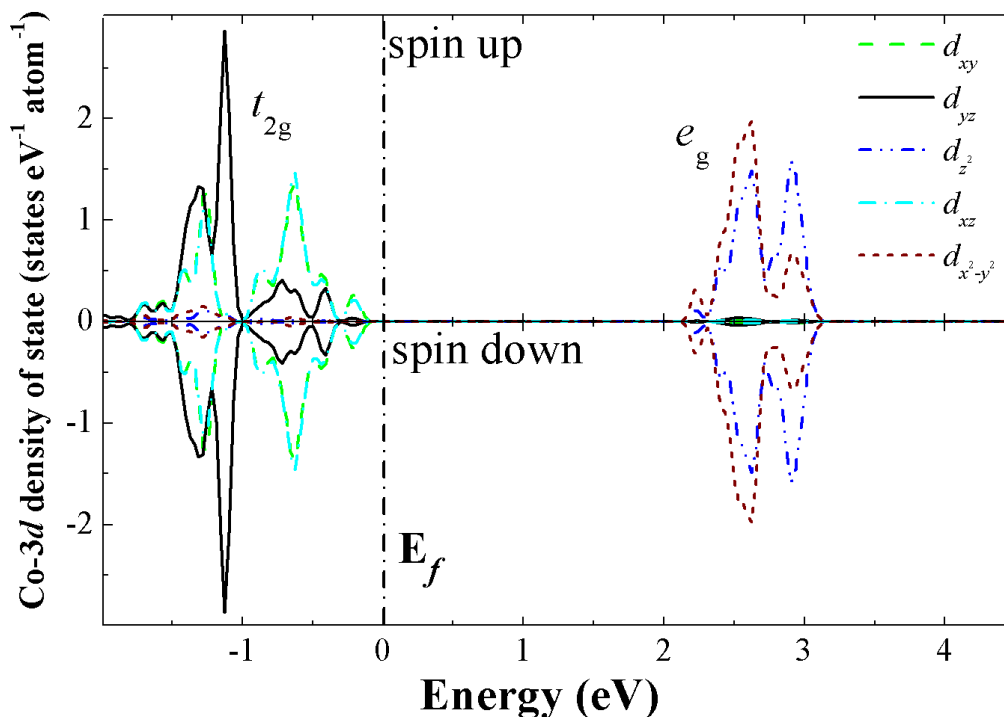


**Figure 2.** Co-3d projected density of states of  $\text{Co}^{3+}$  in  $\text{LiCoO}_2$ . The triplet and doublet of the d-orbitals are denoted as  $t_{2g}$  and  $e_g$ , respectively. The Fermi level is set to 0 eV.

The average oxidation state of the cobalt is  $\text{Co}^{3+}$  in  $\text{LiCoO}_2$ , which corresponds to a  $d^6$  electronic configuration. In an octahedral crystal field, 3d-orbitals split into  $t_{2g}$  triplet and  $e_g$  doublet. As shown in Fig. 2,  $\text{Co}^{3+}$  exhibits a low spin state with 3 electrons occupying the spin up  $t_{2g}$  orbital and the other 3 electrons occupying the spin down  $t_{2g}$  orbital. The energy gap of about 2.4 eV is opened between the occupied  $t_{2g}$  and empty  $e_g$  orbitals. The energy gap is relatively high for activating electrons from the valence band to the conduction band at room temperature. Therefore, the electronic conduction mechanism in  $\text{Li}_x\text{CoO}_2$  should be small polaron migration among  $\text{Co}^{3+}/\text{Co}^{4+}$  ions, in agreement with Goodenough's theory [28].

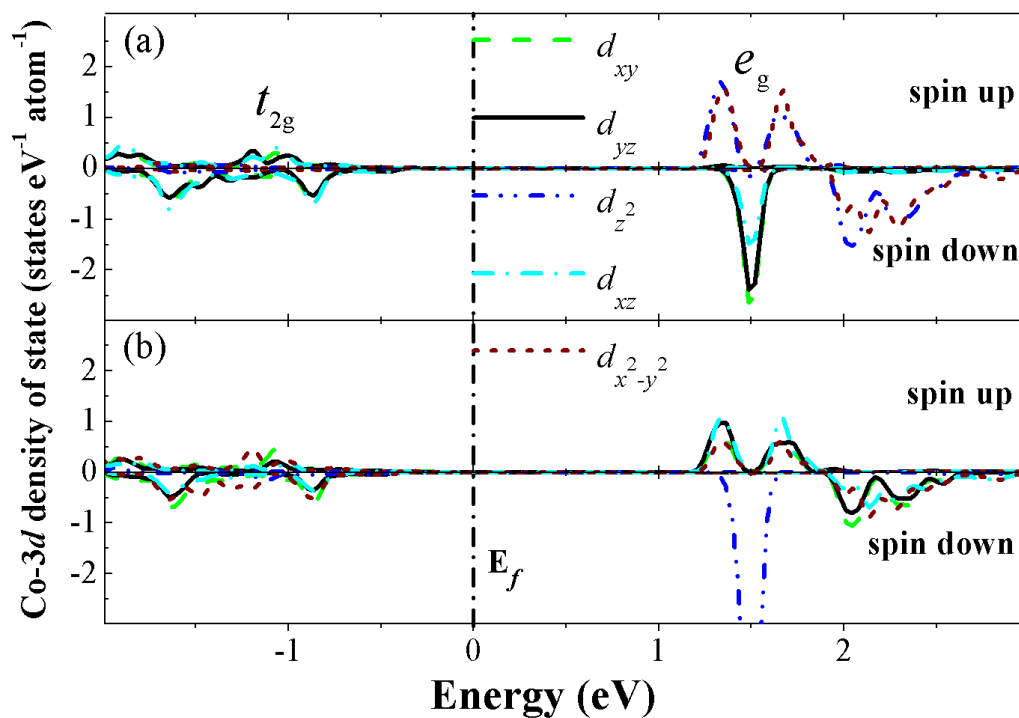


**Figure 3.** Co-3d projected density of states of  $\text{Co}^{4+}$  ions in  $\text{Li}_x\text{CoO}_2$  along the Co-O bond direction (a) and  $c$ -vector direction ( $z$ -axis) of the lattice (b). The five “d-orbitals” in (b) is not really corresponding to the split of an octahedral crystal field. The triplet and the duplet of the d-orbital are denoted as  $t_{2g}$  and  $e_g$ , respectively. The Fermi level is set to 0 eV.

Upon removal of Li atoms from the material, the average cobalt oxidation state is higher than +3, therefore, some Co atoms loss one electron and becomes  $\text{Co}^{4+}$ . After checking the relative positions of  $\text{Co}^{4+}$  and Li vacancies (Li atoms are extracted) in the lattice, we did not observe any correlation among them in our simulation. Meanwhile, the removed Li atoms are not the direct driving force to the formation of  $\text{Co}^{4+}$ , or the distribution of  $\text{Co}^{4+}$  is not related with the distribution of Li vacancies (or the remaining Li atoms) in the lattice. Removal of Li atom from the lattice only accounts for the lost charge in the Co-O layer.

The electronic structure of the  $\text{Co}^{4+}$  3d-state is shown in Fig. 3. Transition from  $\text{Co}^{3+}$  to  $\text{Co}^{4+}$  indicates of removing one electron from the Co-3d orbital. Very interestingly, we found that rather than removing one electron from any one specific orbital from the  $t_{2g}$  triplet ( $d_{xy}$ ,  $d_{yz}$  and  $d_{xz}$ ), the removed electron is contributed by all orbitals of the triplet. This is quite different from Mn and Ni in spinel or layered electrode materials like  $\text{LiMn}_2\text{O}_4$  and  $\text{LiNiO}_2$ . In  $\text{LiMn}_2\text{O}_4$ , transition between  $\text{Mn}^{3+}$  and  $\text{Mn}^{4+}$  is associated with removal of one electron from the  $d(x^2-y^2)$  orbital, which is accompanied by large local distortion of the  $\text{MnO}_6$  octahedral due to the strong Jahn-Teller effect [29]. Similar effect also occurs upon  $\text{Ni}^{3+}/\text{Ni}^{4+}$  transition [30]. In  $\text{LiCoO}_2$ , however, structural distortion around  $\text{Co}^{4+}\text{O}_6$  is much smaller than that of around  $\text{Mn}^{3+}\text{O}_6$  and  $\text{Ni}^{3+}\text{O}_6$ . Since charge is removed from all orbital of the triplet rather than one specific one in the triplet, charge distribution around the  $\text{CoO}_6$  octahedral is quite even around all Co-O bonds, and therefore the bond lengths of all Co-O bonds are similar, which makes the local structure quite stable. As it is shown from Fig. 3a, the charge is contributed almost

equally from all three orbitals. Furthermore, we project the  $\text{Co}^{4+}$ -3d along the  $c$ -vector direction of the lattice ( $z$ -along the  $c$ -vector), and we found that the  $d_{z^2}$  orbital moved up above the Fermi level and become empty (Fig. 3b), indicating that the removed electron is from some kind of “orbital” along the  $c$ -vector direction. In order to confirm this result, Fig. 4 gives the charge density difference  $\Delta\rho$  between  $\text{LiCoO}_2$  and  $\text{Li}_x\text{CoO}_2$  after Li atoms are partly removed. The differential charge density  $\Delta\rho$  is defined as  $\rho(\text{LiCoO}_2) - \rho(\text{Li}_x\text{CoO}_2)$ . Therefore, integration of the  $\Delta\rho$  over the supercell is equal to the number of Li atoms (electrons) removed from the system. As it is shown in Fig. 4, the removed electron from  $\text{Co}^{3+}$  is localized at an “orbital” shaped like  $d_{z^2}$  along the  $c$ -vector, which is consistent with the projected density of states. In the charged state of  $\text{Li}_{0.25}\text{CoO}_2$ , three quarters of the Co ions are in +4, while the other quarter is in +3.

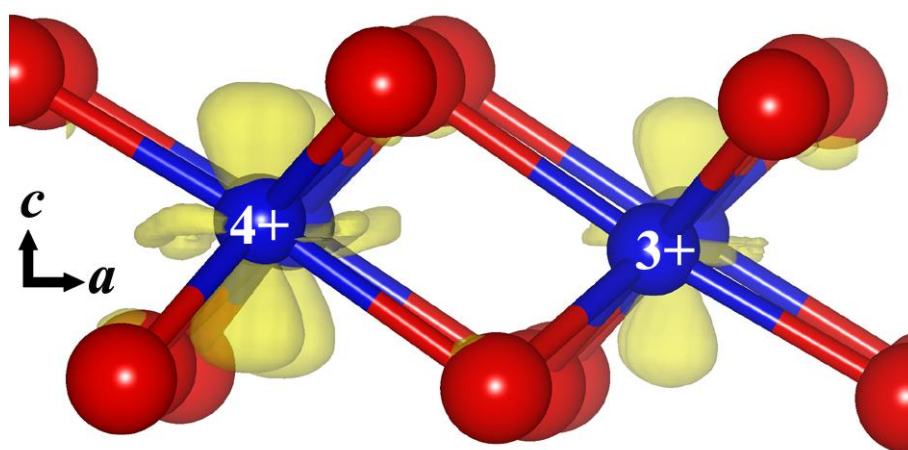


**Figure 4.** Charge density difference between  $\text{LiCoO}_2$  and  $\text{Li}_{0.25}\text{CoO}_2$ . The red (large) and blue (small) balls are O and Co atoms, respectively. Symbols “+4” and “+3” denotes the oxidation state of the corresponding Co atoms, “ $a$ ” and “ $c$ ” refer to the orientation of the lattice vectors.

The above results show that  $\text{CoO}_6$  octahedral structure is quite stable during the lithium insertion/extraction process of the  $\text{LiCoO}_2$  material, because the relatively uniform charge redistribution around the  $\text{CoO}_6$  octahedral upon removal of lithium atoms from the lattice. This is good for the cycling stability of the material as electrodes for lithium ion batteries. The unique charge redistribution around  $\text{CoO}_6$  octahedral is associated with the relative strength between the octahedral crystal field and the exchange correlation of the Co-3d states. The Co atoms in the stoichiometric  $\text{LiCoO}_2$  hold a low-spin  $(t_{2g}\uparrow)^3(t_{2g}\downarrow)^3$  electronic configuration, results in a non-magnetic ground state solution. In the  $\text{Li}_x\text{CoO}_2$  state, some Co ions become  $\text{Co}^{4+}$ , which hold the  $(t_{2g}\uparrow)^3(t_{2g}\downarrow)^2$  electronic configuration and become magnetized with  $1 \mu_B$  magnetic moment. These electronic structures correspond to relatively high structural stability because small local lattice distortion is observed around them. However, the electronic structure and the structural stability may be destroyed by oxygen vacancies, which can be formed upon deep extraction of lithium from the material.

**Table 2.** The local structure and electronic configurations for different types Co ions

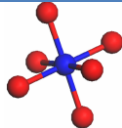
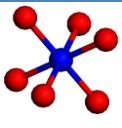
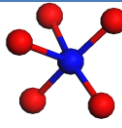
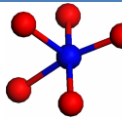
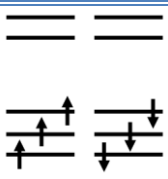
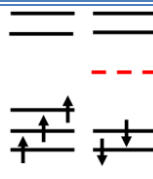
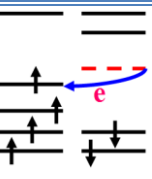
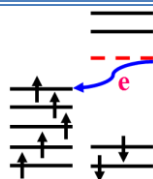
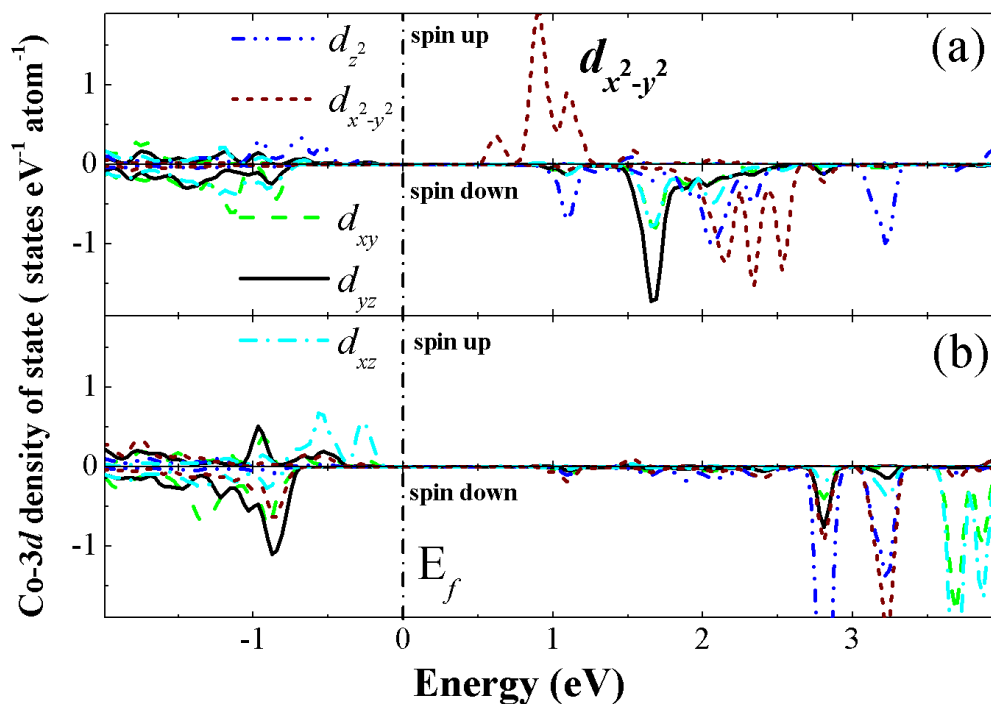
Type of Co ions	Co <sup>3+</sup> in Li <sub>0.75</sub> CoO <sub>2</sub>	Co <sup>4+</sup> in Li <sub>0.75</sub> CoO <sub>2</sub>	Co <sup>3+</sup> around O vacancy in Li <sub>0.75</sub> CoO <sub>2</sub>	Co <sup>2+</sup> around O vacancy in Li <sub>0.75</sub> CoO <sub>2</sub>
Magnetic moments of Co (in $\mu_B$ )	0	1	2	3
Local structures around Co				
Co-O bond lengths (in Å)	1.940 1.963 1.943 1.950 1.967 1.940	1.891 1.890 1.882 1.886 1.886 1.887	1.885 1.886 1.877 1.941 2.009	2.073 1.984 2.122 2.009 1.941
Electronic configurations	$(t_{2g}\uparrow)^3(t_{2g}\downarrow)^3$	$(t_{2g}\uparrow)^3(t_{2g}\downarrow)^2$	$(\uparrow)^4(\downarrow)^2$	$(\uparrow)^5(\downarrow)^2$
				

Fig. 5 gives the electronic structures of Co ions near the O-vacancy. The Co is preferred to be in relatively lower oxidation state. In the case of Li<sub>0.75</sub>CoO<sub>2</sub> with one O vacancy, in addition to Co<sup>3+</sup> ions, we also observed one Co<sup>2+</sup> ion around the O vacancy. Very interestingly, we find that Co<sup>3+</sup> near the O-vacancy is no longer non-magnetic. Spin flip occurs and one spin down electron orbital moves to spin up orbital (see Tab. 2). Because of the O-vacancy, CoO<sub>6</sub> octahedral symmetry is broken and becomes CoO<sub>5</sub>. Therefore, as the crystal field is changed substantially, the Co-O bond lengths and charge distribution are adjusted accordingly. The symmetrical charge distribution around CoO<sub>6</sub>  $(t_{2g}\uparrow)^3(t_{2g}\downarrow)^3$  is changed into  $(\uparrow)^4(\downarrow)^2$ , accompanied with the changed Co-O bond lengths. As a result, the Co<sup>3+</sup> is magnetized with 2  $\mu_B$  magnetic moment (see Tab. 2). Similarly, in addition to one additional electron in the Co-3d orbital, spin flip also occurred in the case of Co<sup>2+</sup> around the O vacancy. The charge distribution is changed from  $(t_{2g}\uparrow)^3(t_{2g}\downarrow)^3$  into  $(\uparrow)^5(\downarrow)^2$ , with which the Co ion has a magnetic moment of 3  $\mu_B$ . After checking the details on the Co-O bond, we can see that the six Co-O bond lengths are quite close to each other around the Co<sup>3+</sup>O<sub>6</sub> in LiCoO<sub>2</sub> and the Co<sup>4+</sup> in Li<sub>1-x</sub>CoO<sub>2</sub> without O vacancies around them, as presented in Tab. 2. Except for the shortened bond length values from ~1.95 Å to 1.89Å, the CoO<sub>6</sub> octahedral do not undergo distortion after one electron removed from Co<sup>3+</sup> and the cation becomes Co<sup>4+</sup>. On the other hand, when there is O vacancy around the Co atom, the Co-O bonds are changed substantially. Even for the case of Co<sup>3+</sup>, spin flip occurs and the bond lengths are no longer close to each other, the CoO<sub>5</sub> structure undergoes substantial distortions. The situation is even more obvious for the case of Co<sup>2+</sup> around the O vacancy. These results suggest that O vacancies play an important role in the structural instability. Upon charging of the LiCoO<sub>2</sub>

cathode to higher voltage, O release is expected and O vacancies are created in the lattice. This in turn further destroys the structural stability, and finally the performance of the material degrades.



**Figure 5.** Co-3d projected density of states of  $\text{Co}^{3+}$  ions (a) and  $\text{Co}^{2+}$  ions (b) next to an O vacancy in  $\text{Li}_{0.75}\text{CoO}_2$ . The project is along the Co-O bond direction. The Fermi level is set to 0 eV.

#### 4. SUMMARY AND CONCLUSIONS

In summary, the atomic and electronic structural changes of  $\text{LiCoO}_2$  cathode material upon delithiation are studied from density functional theory. Upon lithium removal from the  $\text{LiCoO}_2$  lattice, the  $\text{CoO}_6$  structures do not change substantially. The volume expansion is mainly contributed by the lattice expansion along the  $c$ -axis lattice vector, due to the weakened coulomb interactions between positively charged Li layer and negatively charged Co-O layer. As the charge distribution around the  $\text{CoO}_6$  octahedral is quite even, the Co-O bond lengths are close to each other for both  $\text{Co}^{3+}$  and  $\text{Co}^{4+}$  ions. Those results indicate that the structural stability is good upon lithium removal. However, upon high voltage charging of  $\text{LiCoO}_2$ , oxygen release is observed from experiments and oxygen vacancies are formed in the lattice. Oxygen vacancies may induce spin flip to the Co-3d electronic configuration and therefore change the electronic structure and charge distribution substantially, which in turn further distorts the  $\text{CoO}_6$  structure. As a result, oxygen vacancies will accelerate the degradation process of the structural stability, which can possibly create even more vacancies.

## ACKNOWLEDGEMENT

Thanks to the support of NSFC under Grant Nos. 11064004, 11234013 and 11264014. C. Y. Ouyang is also supported by the “Gan-po talent 555” Project of Jiangxi Province. Special thanks to the financial supports from Amperex Technology Limited (ATL) at Ningde, China. Computations are partly performed at Shanghai High Performance Computer center.

## References

1. M. M. Thackeray, W. I. F. David, P. G. Bruce, J. B. Goodenough, *Mat. Res. Bull.*, 18 (1983) 461.
2. J. B. Goodenough, K. Youngsik, *Chem. Mater.*, 22 (2010) 587.
3. R. Koksang, J. Barker, H. Shi, M.Y. Saidi, *Solid State Ionics*. 84 (1996) 1.
4. Y. J. Kim, T. J. Kim, J. W. Shin, B. Park, J. Cho, *J. Electrochem. Soc.*, 149 (2002) A1337.
5. Z. X. Wang, L. J. Liu, L. Q. Chen, X. J. Huang, *Solid State Ionics*, 148 (2002) 335.
6. J. Cho, Y. J. Kim, B. Park, *J. Electrochem. Soc.*, 148 (2001) A1110.
7. A. M. Kannan, L. Rabenberg, A. Manthiram, *Electrochem. Solid-State Lett.*, 6 (2003) A16.
8. L. J. Liu, L. Q. Chen, X. J. Huang, X. Q. Yang, W. S. Yoon, H. S. Lee, J. McBreen, *J. Electrochem. Soc.*, 151 (2004) A1344.
9. A. Van der Ven, M. K. Aydinol, G. Ceder, *Phys. Rev. B*, 58 (1998) 2975.
10. L. Y. Hu, Z. H. Xiong, C. Y. Ouyang, S. Q. Shi, Y. H. Ji, M. S. Lei, Z. X. Wang, H. Li, X. J. Huang, L. Q. Chen, *Phys. Rev. B*, 71 (2005) 125433.
11. M. Catti, *Phys. Rev. B*, 61 (1999) 1795.
12. C. Wolverton and Alex Zunger, *Phys. Rev. Lett.*, 81 (1998) 606.
13. A. Juhin, F. de Groot, *Phys. Rev. B* 81 (2010) 115115.
14. V. I. Anisimov, F. Aryasetiawan, and A. I. Lichtenstein, *J. Phys.: Condens. Mat.* 9 (1997) 767.
15. L. Wang, T. Maxisch, G. Ceder, *Phys. Rev. B* 73 (2006) 195107.
16. C. Y. Ouyang, Y. L. Du, S. Q. Shi, M. S. Lei, *Phys. Lett. A*, 373 (2009) 2796.
17. F. Zhou, M. Cococcioni, C.A. Marianetti, D. Morgan, G. Ceder, *Phys. Rev. B* 70 (2004) 235121.
18. Z. X. Nie, C. Y. Ouyang, J. Z. Chen, Z. Y. Zhong, Y. L. Du, D. S. Liu, S. Q. Shi, and M. S. Lei, *Solid State Commun.*, 150 (2010) 40.
19. G. Kresse, J. Joubert, *Phys. Rev. B* 59 (1999) 1758.
20. G. Kresse, J. Furthmuller, *Phys. Rev. B* 54 (1996) 11169.
21. I. V. Solovyev, P. H. Dederichs, V. I. Anisimov, *Phys. Rev. B*, 50 (1994) 16861.
22. H. J. Monkhorst, J. D. Pack, *Phys. Rev. B* 13 (1976) 5188.
23. L. D. Dyer, B. S. Borie, G. P. Smith, *J. Am. Chem. Soc.* 76 (1954) 1499.
24. J. B. Goodenough, D. G. Wickham, W. J. Croft, *J. Phys. Chem. Solids*, 5 (1958) 107.
25. Y. Takahashia, N. Kijimaa, K. Dokkob, M. Nishizawab, I. Uchidab, J. Akimoto, *J. Solid State Chem.* 180 (2007) 321.
26. M. K. Aydinol, A. F. Kohn, G. Ceder, K. Cho, J. Joannopoulos, *Phys. Rev. B* 56 (1997) 1354.
27. Z. Y. Zhong, C. Y. Ouyang, S. Q. Shi, and M. S. Lei, *ChemPhysChem*, 9 (2008) 2104.
28. J. B. Goodenough, A. Manthiram, B. Wnetrzewski, *J. Power Sources*, 43-44 (1993) 269.
29. C. Y. Ouyang, X. M. Zeng, Z. Sljivancanin, A. Baldereschi, *J. Phys. Chem. C*, 114 (2010) 4756.
30. J. M. Wang, J. P. Hu, C. Y. Ouyang, S. Q. Shi, M. S. Lei, *Solid State Commun.* 151 (2011) 234.